

## ARTICLE OPEN



# Synergistic denitrification mechanism of domesticated aerobic denitrifying bacteria in low-temperature municipal wastewater treatment

Fan Wang<sup>1</sup>, Qin Cui<sup>1</sup>, Wenai Liu<sup>1</sup>, Weiqing Jiang<sup>1</sup>, Shengshu Ai<sup>1</sup>, Wanqi Liu<sup>1</sup> and Dejun Bian<sup>1,2</sup>✉

To address the problems of low efficacy and low microbial activity in low-temperature municipal wastewater treatment, this study utilized an air-lift micro-pressure internal circulation integrated reactor (AMICIR). Through controlling the amount of aeration and dissolved oxygen (DO) in the reactor, AMICIR creates alternating aerobic and anaerobic environments, explores the enrichment conditions of aerobic denitrifying bacteria, examines the changes in pollutant removal efficiency and the characteristics of bacterial colony structure during the process of enrichment of aerobic denitrifying bacteria in the system, and reveals the mechanism of nitrogen removal by aerobic denitrifying bacteria cooperating with anaerobic denitrifying bacteria in the low-temperature municipal wastewater treatment system. Experimental results showed average removal rates of  $\text{NH}_4^+\text{-N}$ , chemical oxygen demand (COD), total phosphorus (TP), and total nitrogen (TN) reaching 93.85%, 89.30%, 92.75%, and 75.4%, respectively. The microorganisms secreted large amounts of proteins and polysaccharides, forming zoogloea and anaerobic microenvironments conducive to traditional denitrification reactions. IlluminaMiSeq sequencing analysis revealed the presence of anaerobic phyla. The system was enriched with a large number of microorganisms, and aerobic denitrifying bacteria (*Flavobacterium*, *Rhodoferrax*, and *Pseudomonas*) were successfully cultured. *Flavobacterium* emerged as the dominant species, with relative abundance ranging from 18.56% to 22.60%. Functional gene prediction indicated high abundance of aerobic denitrification genes, such as *napA*. Aerobic denitrifying bacteria were successfully enriched in the system to improve nitrogen removal from municipal wastewater at low temperatures.

npj Clean Water (2024)7:6; <https://doi.org/10.1038/s41545-024-00299-5>

## INTRODUCTION

The low temperature environment, as an important influencing factor in the biological treatment of wastewater, will delay the expression of denitrification key enzyme genes<sup>1</sup>, inhibit enzyme activity. The expression of nitrite reductase (*nirS*, *narG*) was inhibited by 91% at low temperatures compared to 20–30 °C<sup>2</sup>. The low-temperature environment can disrupt bacterial cell membranes and increase cellular mortality<sup>3</sup>. Slowing down microbial growth, resulting in a significant reduction of denitrification<sup>4</sup>, the temperature was reduced from 25 to 15 °C, and the TN removal rate was reduced from 89% to 60%<sup>5</sup>. Low temperatures also affect the adsorption performance and settling performance of activated sludge<sup>6</sup>. Certain hydrophobic microorganisms compete for acid at low temperatures, resulting in SVI values that are 40–50% higher than in summer<sup>7</sup>. Low temperatures also had a large effect on the treatment of ammonia nitrogen, with removal decreasing from 96% to 70%<sup>8</sup>. The optimal nitrogen removal temperature of most denitrifying bacteria is 25–30 °C<sup>9</sup>, and conventional biological denitrification processes are affected by the low-temperature environment; most of the microorganisms can't metabolize the exogenous substances, resulting in the effect of denitrification of wastewater in the winter becoming worse. The discharged effluent will also make the water quality of the river cross section stink and deteriorate, affecting social production as well as the natural environment on which people depend for their survival. Elimination of the effects of low temperatures is mainly studied through parameter control and the cultivation of cold-tolerant

bacteria. By using an aeration volume of  $0.6 \text{ m}^3 \text{ h}^{-1}$  to control system produces different DO partitions, which leads to good removal results<sup>10</sup>. The long hydraulic retention time (HRT) operation for effective removal of COD and suspended solids (SS), and the removal rates were 74–86% and 86–88%, respectively<sup>11</sup>, to reduce the effect of low temperatures on the system. The biofilm system to cultivate cold-tolerant microorganisms at low temperatures, which improved the stability of the system and made nitrogen removal more effective<sup>12</sup>.

However, this type of method is complex and has a long operating cycle. Aerobic denitrifying bacteria have greater advantages in low-temperature municipal wastewater treatment because of their strong low-temperature<sup>13</sup> and oxygen tolerance<sup>14</sup> and high growth rate<sup>15</sup>. There are fewer studies on aerobic denitrifying bacteria for the treatment of low-temperature municipal wastewater. Aerobic denitrification can produce alkalinity, stabilize the pH of the system<sup>9,16</sup>, and facilitate the removal of inorganic nitrogen<sup>17</sup>. Some bacteria also have heterotrophic nitrification, allowing denitrification and nitrification to occur in a single system. Moreover, aerobic denitrifying bacteria can utilize  $\text{O}_2$  and  $\text{NO}_3^-\text{-N}$  as electron acceptors, and the frequent conversion of aerobic and anaerobic environments is conducive to stimulating the potential of bacteria, improving the removal efficiency of pollutants, and becoming the dominant bacteria in the competition<sup>18</sup>. Some researchers found that *Acinetobacter harbinensis* HITLi7<sup>19</sup>, *Acinetobacter sp.* HA2<sup>20</sup>, and *Pseudomonas putida* Y-9<sup>21</sup> can

<sup>1</sup>Key Laboratory of Urban Sewage Treatment of Jilin Province, Changchun Institute of Technology, Changchun 130012, China. <sup>2</sup>Science and Technology Innovation Center for Municipal Wastewater Treatment and Water Quality Protection, Northeast Normal University, Changchun 130117, China. ✉email: ccgxybiandj@163.com

effectively remove  $\text{NO}_3^-$ -N,  $\text{NO}_2^-$ -N, and  $\text{NH}_4^+$ -N, which provides biotechnological support for nitrogen removal from wastewater at low temperatures. Aerobic denitrification occurs in relation to the DO content gradient, and according to the theory of oxygen mass transfer, there is an aerobic zone on the outside of the zoogloea, and an anoxic and anaerobic zone on the inside<sup>22</sup>. This phenomenon can lead to the simultaneous occurrence of microscopic anaerobic denitrification and aerobic denitrification.

This study designed the unique structure of AMICIR to create an alternating aerobic/anaerobic DO environment. In this way, aerobic denitrifying bacteria were domesticated at low temperatures and synergized with traditional denitrifying bacteria genera to achieve improved effluent treatment efficiency. This paper mainly examines the changes in pollutant removal efficiency during the operation of AMICIR, and analyzes the abundance and diversity of species at different stages. To study the nitrogen metabolism and carbon metabolism pathways of aerobic denitrifying bacteria. To reveal the mechanism of denitrification by aerobic denitrifying bacteria in synergistic manner with anaerobic denitrifying bacteria in the municipal wastewater treatment system. Providing a theoretical basis for aerobic denitrification synergized with anaerobic denitrification

for nitrogen removal in low-temperature municipal wastewater treatment.

## RESULTS AND DISCUSSION

### Analysis of pollutant removal effects

The pollutant removal effects of the AMICIR system at low temperatures for 115 days of continuous operation are shown in Fig. 1. The reactor treatment effect was poor in the initial phase, and Fig. 1a, b illustrates that the treatment effect of COD and  $\text{NH}_4^+$ -N in the system became better after 18 days and 34 days, and was not affected by the change in influent concentration. The microbial abundance increased, and the average COD and  $\text{NH}_4^+$ -N effluent concentrations were  $37.77 \text{ mg L}^{-1}$  and  $1.95 \text{ mg L}^{-1}$ , respectively, which indicated that the carbon source in the system was fully absorbed and utilized by the heterotrophic microorganisms<sup>23</sup>. This is related to the unique structure of the reactor, the formation of three stable cyclones in the reactor greatly extends the movement path of pollutants, able to make the pollutants enter the system and then diffuse to the surrounding area. The system has a high oxygen utilization rate, and COD can be fully utilized in denitrification, which improves the removal of pollutants.

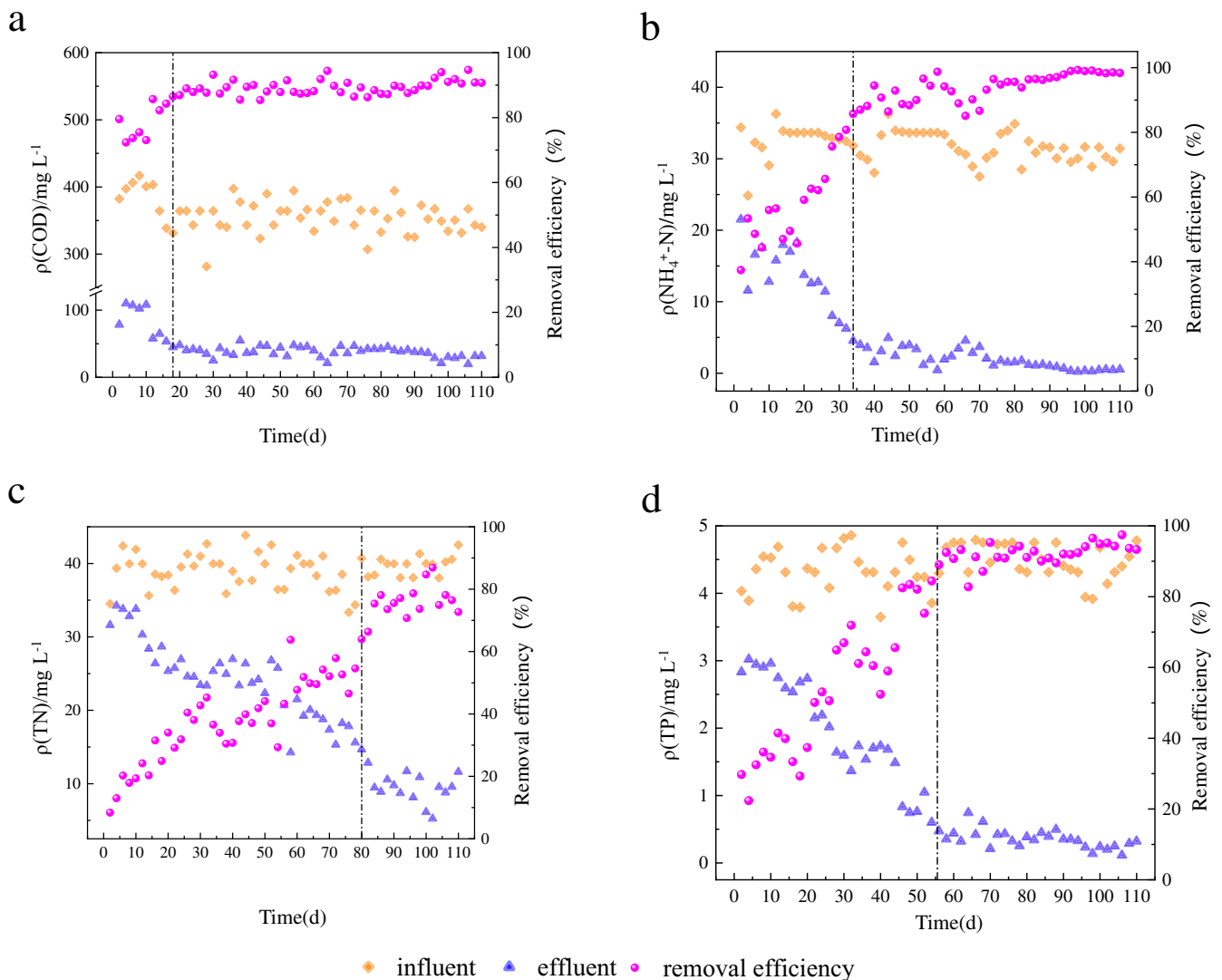


**Fig. 1** Pollutant removal efficiency during system operation. **a** COD; **b**  $\text{NH}_4^+$ -N; **c** TN; and **d** TP.

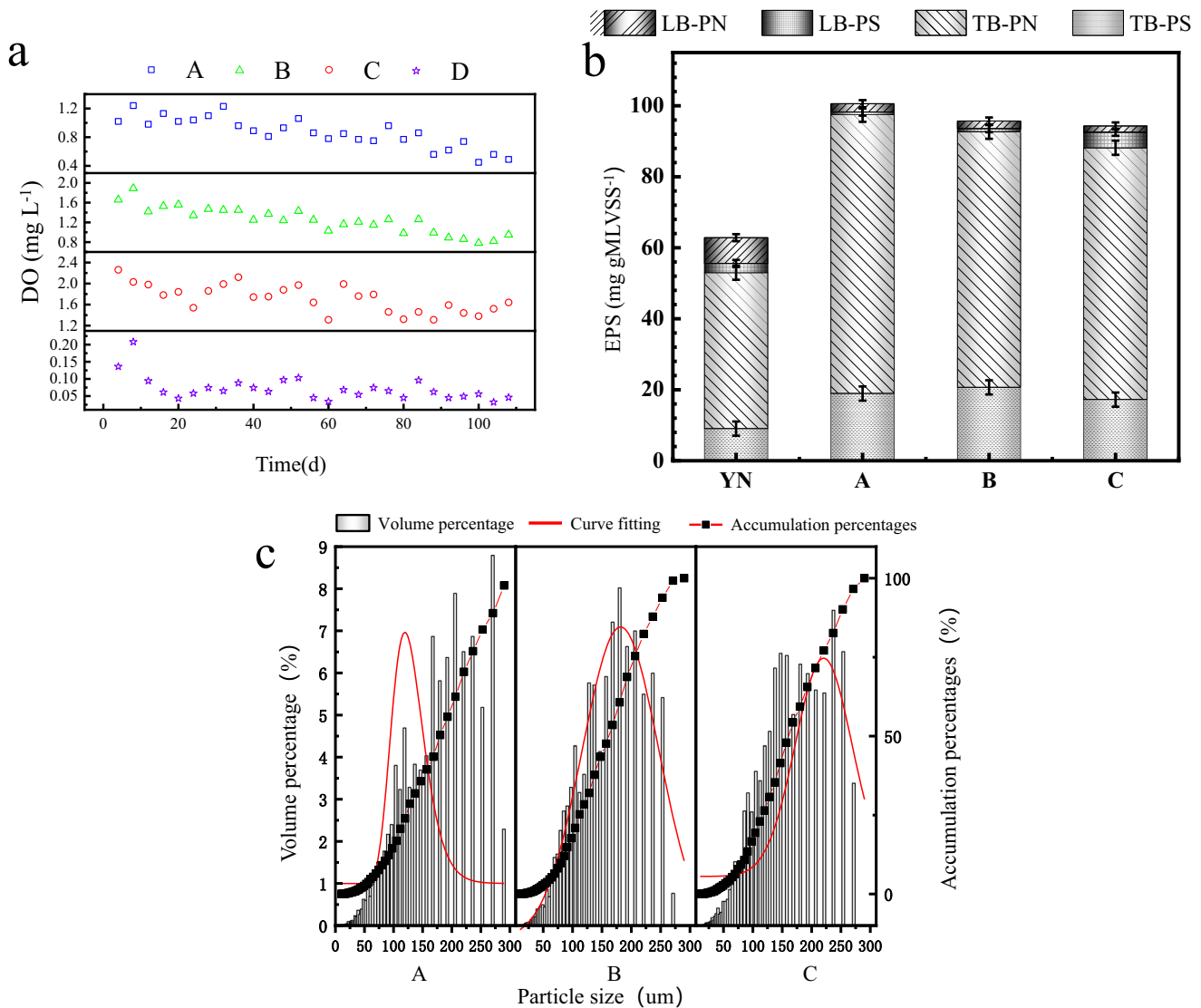


**Fig. 2** System operational characteristics. **a** DO variation of the reactor over the three compartments during operation; **b** EPS variation of the reactor over the three compartments during operation; **c** Particle size variation of the reactor over the three compartments during operation. (The error bars in the figure are all equivalent).

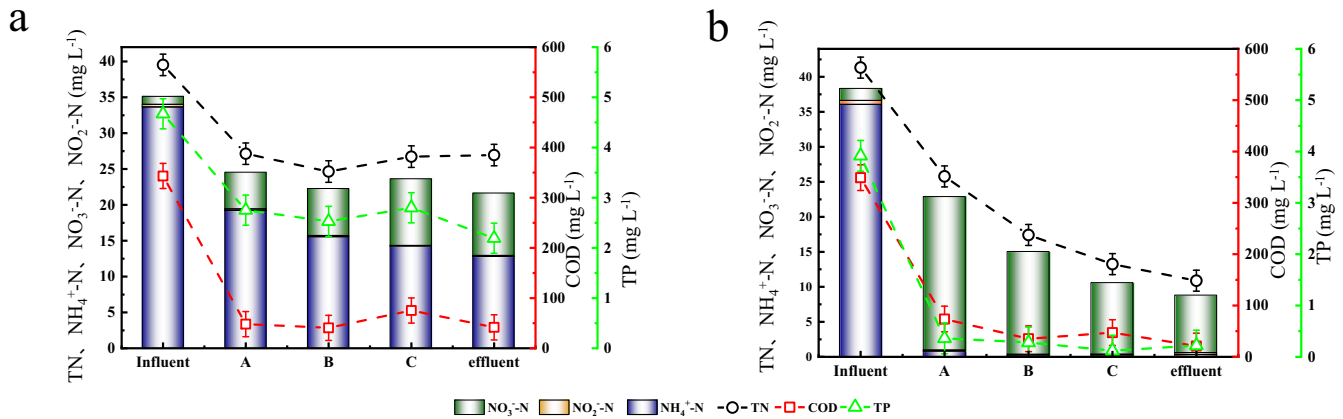
Coupled with the reactor's aerobic environment, nitrification is obvious.

Figure 1c shows the TN removal effect. After 80 days, the TN removal efficiency showed obvious improvement. The microorganisms adapted to the low-temperature environment and grew rapidly, frequently switching between aerobic and anaerobic, which stimulated the potential of functional bacteria. TN in the system reached the standard later than the NH<sub>4</sub><sup>+</sup>-N effluent, nitrifying bacteria adapted to the low-temperature environment with strong ability<sup>24,25</sup>. Cultivation of denitrifying bacteria at low temperatures takes longer. As shown in Fig. 1d, the TP effluent content showed a continuous decreasing trend during the whole system operation period, and the average TP effluent content was reduced to 0.35 mg L<sup>-1</sup> after 58 d. When the denitrification effect in the reactor was improved, the NO<sub>3</sub><sup>-</sup>-N and NO<sub>2</sub><sup>-</sup>-N content in the water and the inhibitory effect on the system decreased<sup>26</sup>, and the average removal rate reached 92.75%. Compared with other (Membrane bioreactors) MBR and partial nitrification-anaerobic ammonia oxidation processes<sup>27,28</sup>, the air-lifted micro-pressure internal recirculation integrated reactor at low temperatures has a more efficient pollutant removal

efficiency and achieves COD and NH<sub>4</sub><sup>+</sup>-N standards earlier. The system was able to have high pollutant removal efficiency at low temperatures, which was related to the structure within the reactor and the dissolved oxygen environment. Functional bacteria were enriched to remove pollutants synergistically and achieved good results.

#### DO distribution and sludge characteristics in the system

The change rule for DO content is shown in Fig. 2a. The average DO content in the center area of the three compartments was 0.87, 1.25, and 1.72 mg L<sup>-1</sup>, which gradually increased along the direction of water flow, mainly because the pollutants were gradually degraded, microorganisms consumed less DO, and the DO content in the B and C biological reaction areas increased. The water-sludge mixture passes through the aerobic biological reaction area of three compartments, A, B, and C, and arrives at reflux channel D, in which the average DO concentration is 0.072 mg L<sup>-1</sup>. The alternating environments of aerobic and anaerobic can stimulate the microorganisms' potential and improve the system's denitrogenation efficiency<sup>29</sup>. As shown in Fig. 2b for the variation of EPS content, the cells secreted more



**Fig. 3** The change pattern of pollutants along the way. The change pattern of COD, NH<sub>4</sub><sup>+</sup>-N, TN, and TP a in 24d and b in 98d. (The error bars in the figure are all equivalent).

proteins and polysaccharides during the stabilization phase (A, B, and C), and the content of TB-EPS in the bioreactivity zones at three compartments was 97.47, 92.71, and 88.18 mg gMLVSS<sup>-1</sup>, respectively. The content of LB-EPS was 3.13, 3.00, and 6.13 mg gMLVSS<sup>-1</sup>, respectively. Figure 2c shows the changes in particle size in the three compartments, mainly observing the particle sizes of D10, D50, and D90 (the cumulative percentage of particle size reaches 10%, 50%, and 90%). The particle size obviously increased in the stabilization stage, and the average values of D10, D50, and D90 were 81.01, 172.88, and 264.76 μm respectively. The system tends to be stabilized, and the cultivation of functional bacteria and domestication are completed. The activated sludge basically matured to form a compact and large activated sludge floc.

EPS, as the basis for the formation of zoogloae<sup>22</sup>, can enable the formation of an anaerobic microenvironment inside the zoogloae and promote denitrification, and the increase of polysaccharides and proteins creates favorable conditions for the formation of zoogloae<sup>30</sup>. Some studies have shown that some functional bacterial genera are able to secrete protective EPS in low-temperature conditions, forming a buffer layer that plays a protective role for the cells against low temperatures<sup>12,31</sup>. As can be seen from the pattern of change in DO and particle size, a larger activated sludge floc is formed in the activated sludge system where the aerobic environment dominates, which is conducive to the generation of an anaerobic microenvironment. It can consume its own carbon source for denitrification in the anaerobic environment inside the bacterial colloid, which improves the denitrification performance of the system.

#### Along-range variation of pollutants in the system

In order to highlight the pollutant removal effect of AMICIR at low temperatures, sludge samples were obtained from three compartments, A, B, and C, at different stages, and the variation along the way in the reactor is shown in Fig. 3. During the initial period of operation (24 d), the effect of nitrogen removal is poor; the contents of COD, NH<sub>4</sub><sup>+</sup>-N, TN, and TP in the effluent are 41.7, 12.75, 26.95, and 2.192 mg L<sup>-1</sup>, respectively. Due to the influence of the low-temperature environment, the functional bacteria have not yet been cultivated successfully, the efficiency of removing the pollutants is low, and the concentration of the pollutants in the three compartments does not vary significantly. The removal of pollutants is mainly realized by the anaerobic microenvironment inside the zoogloea, which is capable of internal denitrification and external nitrification in an environment rich in dissolved oxygen<sup>32</sup>.

System operation to 98d, as shown in Fig. 3b, shows that the system along the course of the pollutant removal law has a

downward trend, the treatment effect is good, the effluent TN and NH<sub>4</sub><sup>+</sup>-N concentrations are 10.88 and 0.22 mg L<sup>-1</sup>, and the systems of nitrifying bacteria and denitrifying bacteria after the enrichment began to play a role. The pollutants were diluted and adsorbed by the water-sludge mixture in A. The NH<sub>4</sub><sup>+</sup>-N was almost completely removed, and the NO<sub>3</sub><sup>-</sup>-N and NO<sub>2</sub><sup>-</sup>-N concentrations were 21.98 and 0.13 mg L<sup>-1</sup>, respectively. This is related to the structure of the reactor, and the inside of the AMICIR is an aerobic environment, and the NH<sub>4</sub><sup>+</sup>-N was all converted to NO<sub>3</sub><sup>-</sup>-N, and the generated NO<sub>3</sub><sup>-</sup>-N was used for assimilation and respiration, with the denitrification function of the bacterial flora playing a role in reducing the TN concentration. Undegraded NO<sub>3</sub><sup>-</sup>-N and part of the activated sludge are driven by water flow into compartment B for further degradation, and NO<sub>3</sub><sup>-</sup>-N may act as electrons for denitrifying phosphorus removal, resulting in lower NO<sub>3</sub><sup>-</sup>-N and TN concentrations. The undegraded pollutants were driven by the water flow into compartment C to enhance the removal, and the TN and NO<sub>3</sub><sup>-</sup>-N content were reduced to 13.25 and 10.26 mg L<sup>-1</sup>, respectively. Finally, the effluent TN and NO<sub>3</sub><sup>-</sup>-N content were further degraded to 10.88 and 8.32 mg L<sup>-1</sup>, respectively. Excellent aerobic absorption of phosphorus took place in the system, and the TP removal rate reached 34.38%. The influent COD concentration is 349.10 mg L<sup>-1</sup>, which provides plenty of carbon sources for denitrification and aerobic phosphorus absorption in this system. Stable cyclonic flow and different DO concentrations in the three biological reaction zones, the anaerobic sedimentation zone, and the unique structure of powerless sludge reflux provide the possibility of simultaneous and efficient removal of NH<sub>4</sub><sup>+</sup>-N, TN, COD, and TP under low-temperature aerobic conditions.

#### Analysis of microbial communities and genes in the reactor

In order to further investigate whether the biological community is associated with pollutant removal, IlluminaMiSeq gene sequencing was used for microbial community analysis. As shown in Table 1, the species richness and diversity in the initial (YN) and stabilization (A, B, C, and D) phases of operation. The experimental results showed that Observed species, Shannon, Simpson, and Chao1 indices were low in the initial phase of operation. The system is affected with the low-temperature environment, which leads to low microbial species and quantities. With the reactor running, the abundance and diversity of microorganisms increased significantly, and sufficient substrate concentration and DO created the conditions for microbial growth. Compared with the YN stage, the species diversity in the stabilization stage showed an increasing trend, which, in combination with the

pollutant removal effect, suggests that a large enrichment of microorganisms is favorable for pollutant removal. It was presumed that the cultivation of functional flora was successful and that a variety of bacterial flora grew synergistically in the system<sup>33</sup>. The microorganisms in the system fully utilized the nutrients, the TN removal effect became better, and it was presumed that the denitrifying bacteria multiplied in large numbers. The microbial abundance and diversity in the reflux channel D were higher, and it was presumed that a better denitrification effect also occurred in the D area, which performed an important role in the whole system. The ASVs index YN and stabilization period were 376 and 355–637, respectively, which also showed the same change rule.

The top 20 bacterial phylum-level abundances within the AMICIR system are shown in Fig. 4a. The four phyla with the highest average relative abundance of the YN, stable phase (A, B, and C) were *Proteobacteria* (49.26%, 48.94%), *Bacteroidetes* (35.58%, 36.78%), *Actinobacteria* (5.74%, 4.00%), and *Acidobacteria* (0.31%, 2.25%). *Proteobacteria* maintained a high abundance in all samples, and *Proteobacteria* were the dominant phylum of microorganisms in the effluent at the phylum level<sup>34</sup>, confirming the presence of an anaerobic environment in the system. *Bacteroidetes* contain a wide range of autotrophic bacteria with nitrogen and phosphorus removal functions that can degrade large amounts of soluble organic carbon such as PN and PS. *Actinobacteria* can play a large role in the denitrification, removal of phosphorus, and degradation of organic matter in wastewater treatment, degrading small molecules of organic matter in anaerobic conditions<sup>35</sup>, and participating in phosphorus uptake under aerobic conditions. Microorganisms of the phylum *Acidobacteria* possess denitrification genes and exhibit corresponding denitrification capacity<sup>36</sup>, which can effectively achieve carbon and nitrogen cycling<sup>37</sup>. Apart from these, the rest of the phyla are relatively less abundant but may also perform an integral role in the system. *Nitrospirae*, *Verrucomicrobia*, and *Gemmatimonadetes*

may be involved in the cycling of nitrogen in the system<sup>38</sup>. *Nitrospirae* (0.00%, 2.26%) is the dominant nitrifying bacteria in low-temperature conditions, which can adapt to sudden cooling<sup>39</sup>, while it is less abundant in the raw sludge, which suggests that the growth of nitrifying bacteria in the system is involved in the low-temperature environment during the experiment.

Figure 4b shows the abundance plot of the 20 most abundant genera during reactor operation. From this figure, the microbial community of the system continuously shifted during the low-temperature operation. The relative abundance of *Chryseobacterium*, *Pseudochrobactrum*, *Rhodobacter*, and *Flavobacterium* in the YN was the highest, with 31.67%, 12.20%, 3.67%, and 2.83%, respectively. When the system was run to the 110th day, the abundance as well as the species of the microbial community shifted considerably under the influence of the low temperature environment, and *Flavobacterium* (18.56%–22.60%) became the dominant species with an increase in abundance. *Flavobacterium* has the aerobic denitrifying function, and some of its species are aerobic denitrifying bacteria<sup>40,41</sup>, the activated sludge switched between anaerobic and aerobic environments, which led to the increase in its abundance and ensured the efficient nitrogen removal in the system, and the large number of dominant bacterial species inhibited the growth of other species, which is consistent with the characterization of the Observed species and the Shannon's index, and the diversity of the biological communities in the system increased, but some of them were reduced in abundance, and the abundant bacterial community in the reactor ensured nitrogen and phosphorus removal, and functional bacterial communities had been successfully cultivated. *Rhodoferrax* (2.25%–3.03%), *Haliangium* (1.76–2.81%), and *Rhodobacter* (1.20%–2.17%)<sup>42,43</sup> are functional bacteria with denitrification and nitrogen fixation under aerobic conditions. *Dechloromonas*<sup>44</sup> (2.41%–3.21%), *Simplicispira*<sup>45</sup> (1.2%–1.54%), and *Thermomonas*<sup>46</sup> (0.68%–1.06%) and others are functional bacteria with denitrification, providing assurance for the denitrification of the system. Typical nitrifying bacteria such as *Niabella* (6.74%–7.18%) and HN-AD bacteria such as *Pseudomonas* (2.14%–2.51%) were also present in the system. The system is capable of cultivating a variety of aerobic denitrifying bacteria to synergistically treat pollutants at low temperatures, and the vast majority of the bacteria have a higher abundance in A. This is mainly due to the unique aeration structure of the reactor, which creates a different DO concentration gradient within the reaction zone, and the richness of the substrate concentration, which provides a suitable environment for the functional bacteria to grow. Microorganisms are also enriched in the reflux channel D. By flowing through the reflux channel to A, the activated sludge switches between anaerobic and aerobic conditions in large quantities and frequently, which contributes to microbial growth as well as

**Table 1.** Richness and diversity of microorganisms communities in activated sludge.

Sample	Observed species	ASVs	Chao1	Shannon	Simpson	Coverage
YN	628.2	376	660.75	5.8237	0.938312	0.997929
A	1138.8	355	1176.69	8.0029	0.982884	0.997321
B	1343	393	1434.23	8.0385	0.981047	0.995007
C	1420.4	637	1434.27	8.1395	0.980227	0.997321
D	1340.8	395	1465.1	7.9902	0.980869	0.994102

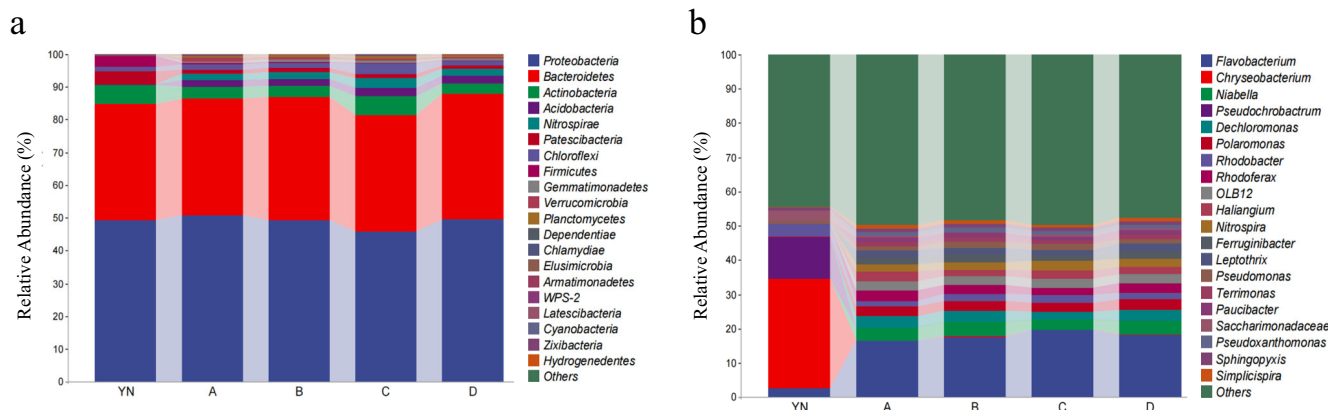


**Fig. 4** Characterization of microflora. Relative abundance of **a** phylum level and **b** genus level at each biota of the reactor.

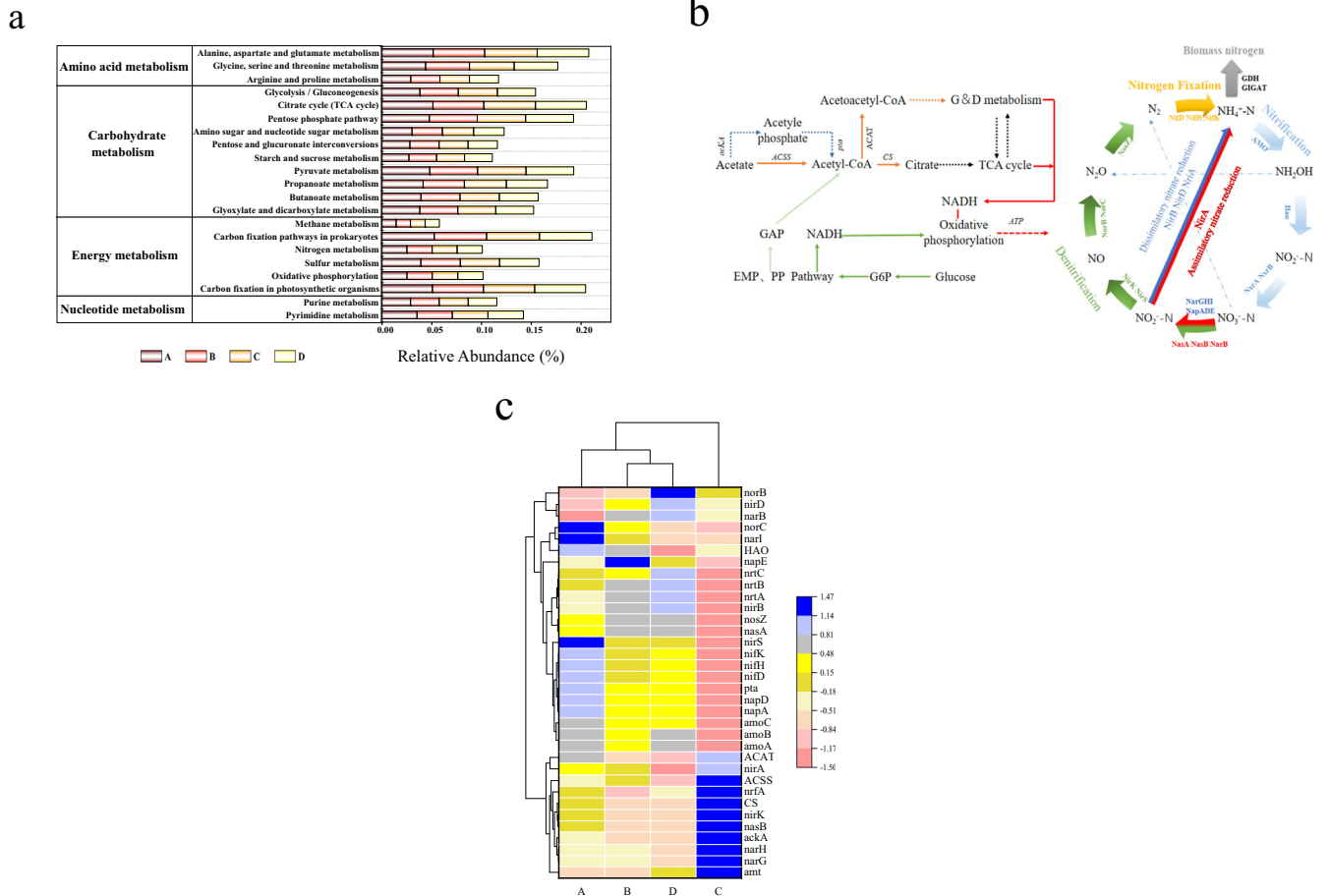


**Fig. 5 Main functions within the system. a** Relative abundance of metabolic subsystems in different compartments of the reactor (percentage per million functional units); **b** Aerobic denitrifying bacterial carbon and nitrogen metabolic pathways; **c** Heat map of functional genes for carbon and nitrogen metabolism at low temperatures.

stimulating the potential of functional bacteria to improve the efficiency of pollutant utilization at low temperatures.

### Functional prediction based on PICRUSt2

In this study, we used the method of PICRUSt2, based on the analysis of metabolic pathway data from the KEGG database, to further investigate which metabolic pathways are involved at low temperatures and to verify that the different reactions occur specifically because of the action of which enzyme system in the cell. As shown in Fig. 5a for sludge samples from the four bioreactor zones A, B, C, and D during the stabilization phase of the system, the abundance of carbohydrate metabolism as well as amino acid metabolism was greater in the functional subsystem (Level 2), which is consistent with the findings of the GUO<sup>47</sup>. The relative abundance of glycolysis/glycolysis, citric acid cycle, pentose phosphate pathway, and pyruvate metabolism in carbohydrate metabolism ensured energy production as well as the synthesis of cellular organisms in the system. The high relative abundance of methane metabolism and nitrogen metabolism demonstrated the presence of methane oxidation and nitrogen pollutant degradation.

There are 6 nitrogen transformation processes and 25 functional genes, such as nitrification, denitrification, and assimilative/isotopic nitrate reduction are shown in Fig. 5a. As shown in Fig. 5c, the heat map of the carbon and nitrogen metabolism genes of aerobic denitrifying bacteria at low temperatures, where the horizontal coordinates of the graph are A, B, D, and C, can be more intuitively

compared with the differences of the same gene at different levels. The low relative abundance of functional genes related to nitrification in the system indicates the existence of another potential pathway for  $\text{NO}_3^-$ -N production and further denitrification. Aerobic denitrification can reduce inorganic nitrogen to gaseous nitrogen, which is more conducive to purifying the water environment. The metabolic pathway of aerobic denitrification is  $\text{NO}_3^-$ -N  $\rightarrow$   $\text{NO}_2^-$ -N  $\rightarrow$   $\text{NO}$   $\rightarrow$   $\text{N}_2\text{O}$   $\rightarrow$   $\text{N}_2$ , and there may also be  $\text{NH}_2\text{OH}$   $\rightarrow$   $\text{N}_2\text{O}$ <sup>48</sup>. Both aerobic denitrification and anaerobic denitrification are capable of denitrification using  $\text{NO}_3^-$ -N reductase (nap, nar, nas),  $\text{NO}_2^-$ -N reductase (nir), NO reductase (nor), and  $\text{N}_2\text{O}$  reductase (nos)<sup>49</sup>. The simultaneous presence of *norB*, *nirK*, *nirS*, and *nosZ* functional genes associated with conventional denitrification ensured nitrogen removal in the system<sup>50</sup>. The alternation of aerobic and anaerobic environments in the reactor facilitates the enrichment of aerobic denitrifying bacteria. Based on the higher TN removal efficiency of the system, the different DO environments, and the variations in microbial colony abundance, it is presumed that there is a synergistic process of aerobic denitrification and anaerobic denitrification in the system. The highest abundance of aerobic denitrifying bacteria was found in A. As the activated sludge flowed through B and C, the abundance of denitrifying genes decreased slightly because of the decrease in substrate concentration and the increase in DO concentration, but the abundance of nitrifying genes showed an increasing trend; the abundance of C was lower than that of D because in the recirculation system, due to the unique structure of the reactor, the flow rate of the activated sludge exchange from C to D was larger, which resulted in a higher

abundance of genes in the reflux channel, and because of the nitrifying liquid reflux, the sludge-water mixture of D then flows to and replenishes A. This cyclic system provides a guarantee for synergistic nitrogen removal by aerobic denitrifying bacteria.

Organic carbon sources provide electrons and energy for the aerobic denitrification process, as shown in Fig. 5b. Several reactions can generate electron donors required for system metabolism, ensuring a good removal effect within the system. The average relative abundance of carbon metabolism function genes within each reaction zone was high, indicating that each compartment had a better carbon metabolism function in low-temperature conditions. From the analysis of the pathway along the way of the reactor, the concentration of TN and COD from C to the effluent water showed a downward trend, and the relative abundance of genes in D was higher, which indicated that the denitrification reaction also occurred in D. D shares the role of TN removal from the system with aerobic denitrifying bacteria.

The results showed that the unique structure of the AMICIR reactor at low temperatures resulted in different DO concentrations in each compartment. The alternating aerobic/anaerobic internal environment promotes the growth and enrichment of aerobic denitrifying bacteria. The microorganisms secrete EPS in large quantities, leading to an increase in the particle size of the activated material sludge, which is conducive to the formation of an anaerobic microenvironment and promotes denitrification effects. Under aerobic conditions, the system successfully domesticated aerobic denitrifying bacteria with the relative abundance of 31.98%~39.02%, and *Flavobacterium* became the dominant species. Aerobic denitrifying bacteria synergized with anaerobic denitrifying bacteria to denitrify nitrogen and achieved

a good effect. The average effluent COD,  $\text{NH}_4^+\text{-N}$ , TN and TP removal rates were 89.30%, 93.85%, 75.4%, and 92.75%, respectively. Functional gene prediction indicated that the enrichment of aerobic denitrification genes, such as *napA*, with denitrification genes, such as *nirK*, *norB*, and *nosZ*, indicated that there was a pathway and function of aerobic denitrification synergizing with anaerobic denitrifying bacteria for denitrification in the system at low temperature. Carbon metabolism provided electron donors and energy for the occurrence of synergism.

## METHODS

### Introduction of the air-lift micro-pressure internal circulation integrated reactor

As shown in Fig. 6, this experiment is an AMICIR device made of plexiglas plates. The size (L×W×H) of AMICIR is 355×100×1120 mm. The total volume is 39.76 L, the effective volume is 39.5 L, and the total reaction area is 27 L. The reactor is split into four parts: A, B, C, and D correspond to the primary, secondary, and tertiary bioreaction areas and the reflux channel, respectively, and the aeration method is perforated aeration. The inlet point, aeration, and sludge reflux are all located in A, with a volume of 9 L. The position of the single-side aeration tube is located at the bottom of A, at the outlet of the reflux channel. The system is oxygenated by aeration, and the bubbles generated can be used as the driving force to drive the water-sludge mixture to form a stable cyclonic flow, and the negative pressure can return the sludge from the reflux channel back to the A, forming a good reflux of sludge and nitrification solution. Bubbles can drive the water-sludge mixture to B, through the role of the top partition to

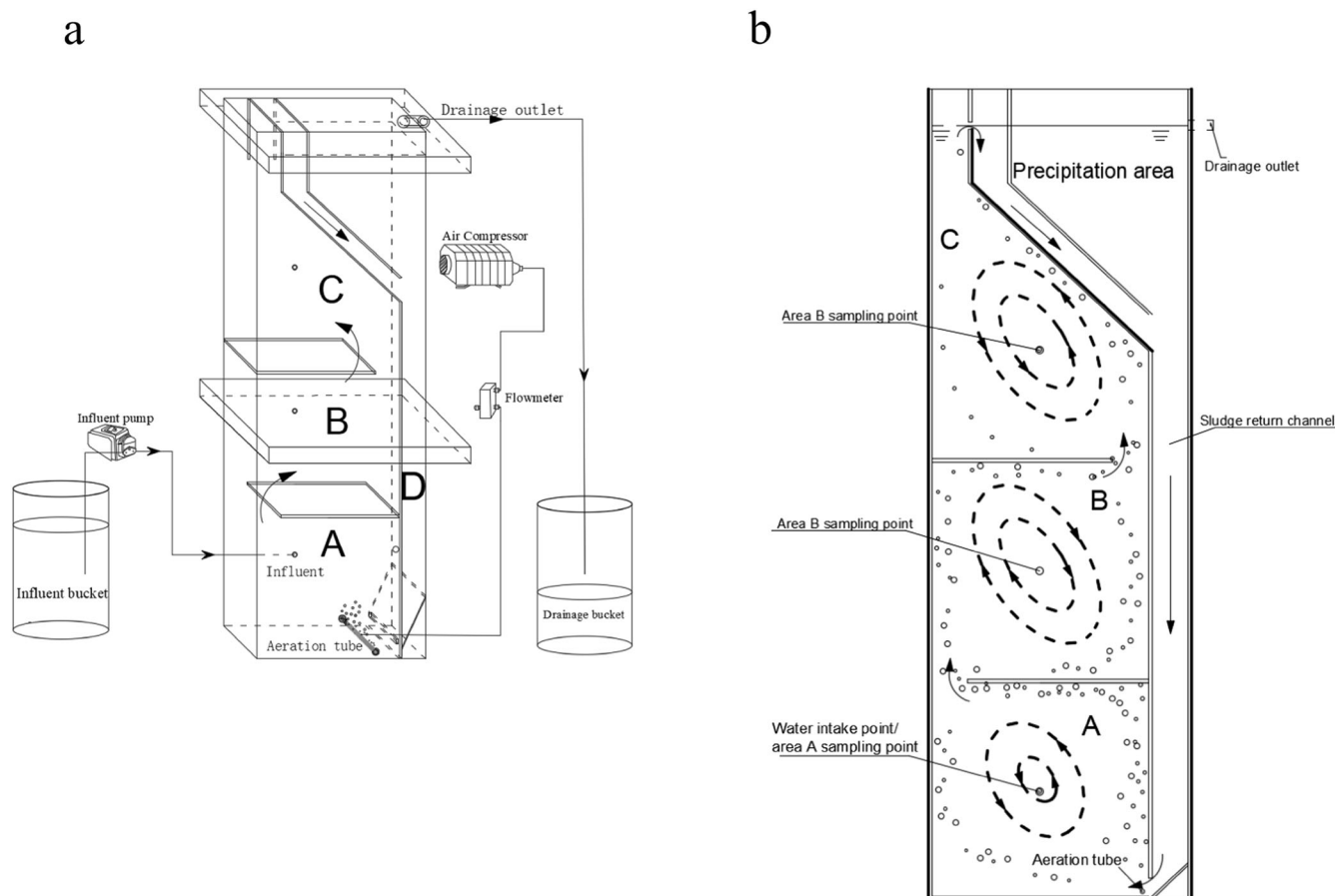


**Fig. 6** Test operation device. **a** Schematic diagram of air-lift micro-pressure internal circulation integrated reactor, **b** Flowchart of air-lift micro-pressure internal circulation integrated reactor.

**Table 2.** Synthetic wastewater quality.

Pollutants	COD (mg L <sup>-1</sup> )	NH <sub>4</sub> <sup>+</sup> -N (mg L <sup>-1</sup> )	TN (mg L <sup>-1</sup> )	TP (mg L <sup>-1</sup> )	pH
Range	281.40–416.90	27.50–36.27	33.34–43.85	3.65–4.86	7.35–8.42
Average value	359.37	31.89	37.18	4.41	7.82

form a better circulation in the internal B for further removal of pollutants, and the volume of 9 L. C for further removal of ammonia nitrogen and removal of organic matter, and the volume of 11.4 L. After the treatment of sewage flow to the sedimentation tank, sludge-water separation, supernatant discharged out of the system through the role of the overflow, activated sludge sludge through the role of sedimentation through the D (return channel), which is circulated to the system.

### Original sludge and experimental water quality

The activated sludge was collected from the tail section of biochemical pond in a municipal wastewater treatment plant in Changchun, Jilin Province, China, with good wastewater treatment performance. It was obtained from the wastewater plant in winter and injected into the system after removing the larger particles of residue through a screen mesh, and the initial sludge content of the system was controlled at (4700 ± 200) mg L<sup>-1</sup>.

The water used for operation in the system was simulated municipal wastewater at low temperatures, in which COD was mainly provided by soluble starch and CH<sub>3</sub>COONa, NH<sub>4</sub><sup>+</sup>-N was mainly provided by NH<sub>4</sub>Cl, and TP was mainly provided by KH<sub>2</sub>PO<sub>4</sub>. The purity of the above reagents was analytically pure (Tianjin Guangfu Pharmaceutical Factory), and some beef paste and peptone (Beijing Aoboxing) were also used to provide COD, NH<sub>4</sub><sup>+</sup>-N, and TP. The specific influent water quality and pH during the experiment are shown in Table 2.

### Operating parameter setting and equipment start-up

The AMICIR was operated with continuous water intake; the experiment was carried out at low temperatures, and the water temperature was stabilized at about 10 °C by controlling the air temperature. HRT was 12 h, the aeration was (1±0.05) m<sup>3</sup>/h, the influent flow rate was 2.25 L/h, the sludge retention time was 30 d, the amount of sludge discharged from the reactor was 0.9 L/d daily, and the aeration was controlled by a glass rotameter. The total reactor operation time is 115 d, and the effluent concentrations of COD, TP, and NH<sub>4</sub><sup>+</sup>-N were stable after 56 d of sludge domestication, and stabilization of TN concentration in effluent after 80 d. All the indexes during the stable operation were better than the Class A discharge standard of the Emission Standard for Pollutants from Urban Wastewater Treatment Plants (GB18918-2002).

### Analysis methods

AMICIR system effluent water sample detection method: COD was determined by the potassium dichromate method (5B-1, Lian-hua Tech. Co., Ltd., China); NH<sub>4</sub><sup>+</sup>-N, TN, and TP were determined and analyzed by the Nesler reagent spectrophotometric method, the alkaline potassium persulfate elimination method, and the ammonium molybdate spectrophotometric method, respectively. The filtered water samples were then passed through a 0.22 μm filter and used for the determination of nitrate and nitrite nitrogen by ion chromatography (881 compact ICpro, Metrohm, Switzerland); DO was determined by a portable dissolved oxygen meter (Multi340i, WTW, Germany); pH was measured by a Remagnet acidity meter (PHSJ-4A, Lei Ci, Shanghai, China); and the particle size was determined by a laser particle size analyzer. Proteins (PN) and polysaccharides (PS) in extracellular polymeric substances (EPS) were determined by the Folin-phenol reagent method and the anthrone method.

The EPS was extracted by taking 30 ml of the sludge mixture from three compartments of the reactor, centrifuging at 4000 r for 5 min, discarding the supernatant, adding 9 mL of 0.05% NaCl solution and stirring well. Then take the 0.05% NaCl solution heated at 70 °C and fixed to 30 ml. Finally, after centrifuging at 4000 r for 10 min, the organic material extracted from the supernatant is loosely bound EPS (LB-EPS). The remaining sludge after extraction is restored to the initial volume of 30 ml with 0.05% NaCl solution, and the mixture is then heated in a water bath at 60 °C for 30 min, followed by centrifugation at 4000 r for 15 min. The supernatant is tightly bound EPS (TB-EPS).

Activated sludge samples were collected in four zones A, B, C, and D of the AMICIR. The sampling times were when the system was operated up to the 2nd day (YN) and the 98th day (stabilization phase), respectively, and 5 ml of each sample was taken and stored in a storage tube at -80 °C in a refrigerator. Total genomic DNA was extracted using a kit (omega), and DNA integrity was analyzed by the agarose gel method. The libraries were first quantified using the Agilent High Sensitivity DNA Kit, then the Quant-iT Micro dsDNA Quantification Kit on an original quantitative fluorescence quantification system, gradient diluted, and then sequenced using a MiSeq sequencer.

The abundance of sample KEGG homologous genes and EC enzymes was predicted by PICRUSt2. The metabolic pathways of organic matter and nitrogen were inferred from the abundance of metabolic pathways and functional genes<sup>51</sup>.

### DATA AVAILABILITY

The datasets derived from this work are available from the corresponding author upon reasonable request.

Received: 11 September 2023; Accepted: 19 January 2024;

Published online: 05 February 2024

### REFERENCES

- Morales, N. et al. The Granular Biomass Properties And The Acclimation Period Affect The Partial Nitrification/Anammox Process Stability At A Low Temperature And Ammonium Concentration. *Process Biochem.* **51**, 2134–2142 (2016).
- Saleh-Lakha, S. et al. Effect Of Ph And Temperature On Denitrification Gene Expression And Activity In *Pseudomonas Mandelii*. *Appl. Environ. Microbiol.* **75**, 3903–3911 (2009).
- Pham, H. T. et al. Enhancing Biochar Structure And Removal Efficiency Of Ammonium And Microalgae In Wastewater Treatment Through Combined Biological And Thermal Treatments. *J. Water Process Eng.* **56**, 104529 (2023).
- Johnston, J. T. & Lapara, S. Behrens. Composition And Dynamics Of The Activated Sludge Microbiome During Seasonal Nitrification Failure. *Sci. Rep.* **9**, 4565 (2019).
- Cai, Y. et al. Wastewater Treatment For Ships Experiencing Large Temperature Changes: The Activated Sludge/Membrane-Biofilm Reactor. *Chemosphere* **307**, 135852 (2022).
- Zhang, J., Wu, P., Hao, B. & Yu, Z. Heterotrophic Nitrification And Aerobic Denitrification By The Bacterium *Pseudomonas Stutzeri* Yzn-001. *Bioresour. Technol.* **102**, 9866–9869 (2011).
- Deepnarain, N. et al. Decision Tree For Identification And Prediction Of Filamentous Bulking At Full-Scale Activated Sludge Wastewater Treatment Plant. *Process Saf. Environ. Prot.* **126**, 25–34 (2019).
- Nancharaiyah, Y. V. & Sarvajith, M. Granular Stability, Nitrogen And Phosphorus Removal Pathways Of Aerobic Granular Sludge Treating Real Municipal Wastewater At Different Temperatures. *J. Environ. Chem. Eng.* **11**, 110769 (2023).
- Ji, B. et al. Aerobic Denitrification: A Review Of Important Advances Of The Last 30 Years. *Biotechnol. Bioprocess Eng.* **20**, 643–651 (2015).



10. Ai, S. et al. Characterization Of A Novel Micro-Pressure Double-Cycle Reactor For Low Temperature Municipal Wastewater Treatment. *Environ. Technol.* **44**, 394–406 (2023).
11. Laura, D. et al. The Influence Of Lower Temperature, Influent Fluctuations And Long Retention Time On The Performance Of An Upflow Mode Laboratory-Scale Septic Tank. *Desalination Water Treat.* **57**, 18679–18687 (2016).
12. Zhang, J. et al. Mechanism Of Stable Sewage Nitrogen Removal In A Partial Nitrification-Anammox Biofilm System At Low Temperatures: Microbial Community And Eps Analysis. *Bioresour. Technol.* **297**, 122459 (2020).
13. Wang, L., Chen, C., Tang, Y. & Liu, B. Efficient Nitrogen Removal By A Novel Extreme Strain, *Pseudomonas Reactans* W120-3 Under Dual Stresses Of Low Temperature And High Alkalinity: Characterization, Mechanism, And Application. *Bioresour. Technol.* **385**, 129465 (2023).
14. Lu, Z. et al. Iron-Based Multi-Carbon Composite And *Pseudomonas Furukawaii* Zs1 Co-Affect Nitrogen Removal, Microbial Community Dynamics And Metabolism Pathways In Low-Temperature Aquaculture Wastewater. *J. Environ. Manag.* **349**, 119471 (2024).
15. Hu, Y. et al. Comparative Genomic Analysis Of Two Arctic *Pseudomonas* Strains Reveals Insights Into The Aerobic Denitrification In Cold Environments. *Bmc Genomics.* **24**, 534 (2023).
16. Srivastava, G. & Kazmi, A. A. Role Of Ammonia Oxidizers In Performing Simultaneous Nitrification And Denitrification Process In Advanced Sbr Plants. *Dev. Wastewater Treat. Res.* **229**, 347–370 (2022).
17. Sui, Y., Cui, Y. W., Huang, J. L. & Xu, M. J. Feast/Famine Ratio Regulates The Succession Of Heterotrophic Nitrification-Aerobic Denitrification And Autotrophic Ammonium Oxidizing Bacteria In Halophilic Aerobic Granular Sludge Treating Saline Wastewater. *Bioresour. Technol.* **393**, 129995 (2023).
18. Bucci, P. et al. Heterotrophic Nitrification-Aerobic Denitrification Performance In A Granular Sequencing Batch Reactor Supported By Next Generation Sequencing. *Int. Biodeterior. Biodegrad.* **160**, 105210 (2021).
19. Zheng, Z. et al. Substrates Removal And Growth Kinetic Characteristics Of A Heterotrophic Nitrifying-Aerobic Denitrifying Bacterium, *Acinetobacter Harbinensis* Hitli<sup>T</sup> At 2°C. *Bioresour. Technol.* **259**, 286–293 (2018).
20. Yao, S., Ni, J., Chen, Q. & Borthwick, A. G. Enrichment And Characterization Of A Bacteria Consortium Capable Of Heterotrophic Nitrification And Aerobic Denitrification At Low Temperature. *Bioresour. Technol.* **127**, 151–157 (2013).
21. Xu, Y. et al. Nitrogen Removal Characteristics Of *Pseudomonas Putida* Y-9 Capable Of Heterotrophic Nitrification And Aerobic Denitrification At Low Temperature. *Biomed. Res. Int.* **2017**, 1–7 (2017).
22. An, W., Guo, F. & Song, Y. Comparative Genomics Analyses On Eps Biosynthesis Genes Required For Floc Formation Of *Zoogloea Resiniphila* And Other Activated Sludge Bacteria. *Water Res.* **102**, 494–504 (2016).
23. Guo, Y. et al. Effects Of Hydraulic Retention Time (Hrt) On Denitrification Using Waste Activated Sludge Thermal Hydrolysis Liquid And Acidogenic Liquid As Carbon Sources. *Bioresour. Technol.* **224**, 147–156 (2017).
24. Li, R. et al. Sequential Adaptation Strategies Of Spda Systems To Low Temperature: Eps Mediation And Community Structure Evolution. *J. Clean. Prod.* **425**, 138850 (2023).
25. Peng, Z. et al. Exploring And Comparing The Impacts Of Low Temperature To Endogenous And Exogenous Partial Denitrification: The Nitrite Supply, Transcription Mechanism, And Microbial Dynamics. *Bioresour. Technol.* **370**, 128568 (2023).
26. Shao, L. et al. Advance In The Sulfur-Based Electron Donor Autotrophic Denitrification For Nitrate Nitrogen Removal From Wastewater. *World J. Microbiol. Biotechnol.* **40**, 7–7 (2023).
27. Lagum, A. A., Ghriybah, A. M. & Ma'abreh, A. A. Coupling Membrane Electro-Bioreactor With Anammox Process To Treat Wastewater At Low Temperatures. *Arab. J. Chem.* **16**, 105165 (2023).
28. Jia, T. et al. Advanced Nitrogen Removal From Municipal Sewage Via Partial Nitrification-Anammox Process Under Two Typical Operation Modes And Seasonal Ambient Temperatures. *Bioresour. Technol.* **363**, 127864 (2022).
29. Wang, F. et al. Simultaneous Removal Of Organic Matter And Nitrogen By Heterotrophic Nitrification-Aerobic Denitrification Bacteria In An Air-Lift Multi-Stage Circulating Integrated Bioreactor. *Bioresour. Technol.* **363**, 127888 (2022).
30. Wang, J. Y. et al. The Acceleration Of Aerobic Sludge Granulation By Alternating Organic Loading Rate: Performance And Mechanism. *J. Environ. Manag.* **347**, 119047 (2023).
31. Liu, C. et al. Nitrogen Removal Performance And Microbial Community Changes In Subsurface Wastewater Infiltration Systems (Swiss) At Low Temperature With Different Bioaugmentation Strategies. *Bioresour. Technol.* **250**, 603–610 (2018).
32. Li, J. et al. Denitrification Performance And Mechanism Of Sequencing Batch Reactor With A Novel Iron-Polyurethane Foam Composite Carrier. *Biochemical Eng. J.* **176**, 108209 (2021).
33. Shannon, C. E. A Mathematical Theory Of Communication. *Bell Syst. Tech. J.* **27**, 379–423 (1948).
34. Zhang, T., Shao, M. F. & Ye, L. 454 Pyrosequencing Reveals Bacterial Diversity Of Activated Sludge From 14 Sewage Treatment Plants. *Isme J.* **6**, 1137–1147 (2012).
35. Zhao, Y. et al. Effect Of Different Salinity Adaptation On The Performance And Microbial Community In A Sequencing Batch Reactor. *Bioresour. Technol.* **216**, 808–816 (2016).
36. Liao, R. et al. Performance And Microbial Diversity Of An Expanded Granular Sludge Bed Reactor For High Sulfate And Nitrate Waste Brine Treatment. *J. Environ. Sci.* **26**, 717–725 (2014).
37. Eichorst, S. A. et al. Genomic Insights Into The *Acidobacteria* Reveal Strategies For Their Success In Terrestrial Environments. *Environ. Microbiol.* **20**, 1041–1063 (2018).
38. Wertz, J. T. et al. Genomic And Physiological Characterization Of The *Verrucomicrobia* Isolate *Diplosphaera Colitermitum* Gen. Nov., Sp. Nov., Reveals Microaerophily And Nitrogen Fixation Genes. *Appl. Environ. Microbiol.* **78**, 1544–1555 (2012).
39. Chen, M. et al. Mixed Nitrifying Bacteria Culture Under Different Temperature Dropping Strategies: Nitrification Performance, Activity, And Community. *Chemosphere* **195**, 800–809 (2018).
40. Chen, J. et al. Start-Up And Microbial Communities Of A Simultaneous Nitrogen Removal System For High Salinity And High Nitrogen Organic Wastewater Via Heterotrophic Nitrification. *Bioresour. Technol.* **216**, 196–202 (2016).
41. Pishgar, R., Dominic, J. A., Sheng, Z. & Tay, J. H. Denitrification Performance And Microbial Versatility In Response To Different Selection Pressures. *Bioresour. Technol.* **284**, 72–83 (2019).
42. Gweon, H. S. et al. Contrasting Community Assembly Processes Structure Lotic Bacteria Metacommunities Along The River Continuum. *Environ. Microbiol.* **23**, 484–498 (2021).
43. McIlroy, S. J. et al. Identification Of Active Denitrifiers In Full-Scale Nutrient Removal Wastewater Treatment Systems. *Environ. Microbiol.* **18**, 50–64 (2016).
44. Wang, X. et al. Evaluating The Potential For Sustaining Mainstream Anammox By Endogenous Partial Denitrification And Phosphorus Removal For Energy-Efficient Wastewater Treatment. *Bioresour. Technol.* **284**, 302–314 (2019).
45. Siddiqi, M. Z. et al. *Simplicispira Hankyongi* Sp. Nov., A Novel Denitrifying Bacterium Isolated From Sludge. *Antonie Van. Leeuwenhoek.* **113**, 331–338 (2020).
46. Xing, W. et al. Stable-Isotope Probing Reveals The Activity And Function Of Autotrophic And Heterotrophic Denitrifiers In Nitrate Removal From Organic-Limited Wastewater. *Environ. Sci. Technol.* **52**, 7867–7875 (2018).
47. Guo, J. et al. Unraveling Microbial Structure And Diversity Of Activated Sludge In A Full-Scale Simultaneous Nitrogen And Phosphorus Removal Plant Using Metagenomic Sequencing. *Enzym. Microb. Technol.* **2017**, 102 (2017).
48. Zhang, Y. et al. Optimization Of Nitrogen Removal Conditions Based On Response Surface Methodology And Nitrogen Removal Pathway Of *Paracoccus* Sp. Qd-19. *Sci. Total Environ.* **908**, 168348 (2024).
49. Ruan, Y. et al. Performance Of Aerobic Denitrification By The Strain *Pseudomonas Balearica* Rad-17 In The Presence Of Antibiotics. *Microorganisms* **9**, 1584 (2021).
50. Ruan, Y. et al. Kinetic Affinity Index Informs The Divisions Of Nitrate Flux In Aerobic Denitrification. *Bioresour. Technol.* **309**, 123345 (2020).
51. Zhang, S. et al. Heterotrophic Nitrification And Aerobic Denitrification By *Diaphorobacter Polyhydroxybutyrativorans* SI-205 Using Poly(3-Hydroxybutyrate-Co-3-Hydroxyvalerate) As The Sole Carbon Source. *Bioresour. Technol.* **241**, 500–507 (2017).

## ACKNOWLEDGEMENTS

The research was funded by the Jilin Province Science and Technology Development Program (YDZJ202201ZYT5638).

## AUTHOR CONTRIBUTIONS

Fan Wang: Writing - Review & Editing, Investigation, Formal analysis, Resources, Supervision. Qin Cui: Methodology, Formal analysis, Visualization, Writing - Original Draft, Conceptualization. Wenai Liu: Writing - Review & Editing, Visualization. Weiqing Jiang: Investigation, Formal analysis. Shengshu Ai: Investigation, Supervision. Wanqi Liu: Formal analysis, Writing - Review & Editing. Dejun Bian: Supervision, Writing - Review & Editing.

## COMPETING INTERESTS

The authors declare no competing interests.

## ADDITIONAL INFORMATION

**Correspondence** and requests for materials should be addressed to Dejun Bian.

**Reprints and permission information** is available at <http://www.nature.com/reprints>

**Publisher's note** Springer Nature remains neutral with regard to jurisdictional claims in published maps and institutional affiliations.



**Open Access** This article is licensed under a Creative Commons Attribution 4.0 International License, which permits use, sharing, adaptation, distribution and reproduction in any medium or format, as long as you give appropriate credit to the original author(s) and the source, provide a link to the Creative Commons license, and indicate if changes were made. The images or other third party material in this article are included in the article's Creative Commons license, unless indicated otherwise in a credit line to the material. If material is not included in the article's Creative Commons license and your intended use is not permitted by statutory regulation or exceeds the permitted use, you will need to obtain permission directly from the copyright holder. To view a copy of this license, visit <http://creativecommons.org/licenses/by/4.0/>.

© The Author(s) 2024